Dipole momenta and compositeness of the τ lepton at Belle II

M. Fabbrichesi[1] and L. Marzola[2]

[1]*INFN, Sezione di Trieste, Via Valerio 2, I-34127 Trieste, Italy*

[2]*Laboratory of High-Energy and Computational Physics, NICPB, Rävala 10, 10143 Tallinn, Estonia*

(Received 15 January 2024; accepted 19 April 2024; published 20 May 2024)

The large number of τ leptons available at the Belle II experiment makes it possible to study their properties and the extent of their compositeness. We propose a strategy that relies on three observables defined in terms of elements of the polarization density matrix of the produced τ pairs, which we obtain via quantum tomography. We find that these observables can explore values of the magnetic dipole moment down to 6.3×10^{-4}, which is 2 orders of magnitude better than the current experimental limit, constrain the electromagnetic radius below 4.3×10^{-3} fm, and exclude an electric dipole moment larger than 1.7×10^{-17} e cm. The quoted limits are at the 95% confidence level (CL) and are obtained for a benchmark integrated luminosity of 1 ab^{-1} and a Monte Carlo estimate of the statistical sensitivity.

DOI: 10.1103/PhysRevD.109.095026

I. INTRODUCTION

The abundant production of τ-lepton pairs in $e^+e^- \to \tau^+\tau^-$ at Belle II [1] provides a promising laboratory for a systematic analysis of their electromagnetic couplings. The study is important because deviations of these parameters from their Standard Model (SM) values would provide insights into the nature of underlying new physics, implying, for instance, the presence of new particles or interactions. Given the current data, the τ lepton—the heaviest among the leptons, as the top quark among the quarks—could be the likeliest to show a behavior departing from that described by the SM. In this paper, we then investigate the electric dipole moment, the anomalous magnetic moment, and the possible substructure of the τ lepton, represented by the size of its radius that we define below.

The most general electromagnetic Lorentz-invariant coupling between the photon (with momentum q) and the τ lepton can be written as

$$-ie\bar{\tau}\Gamma^{\mu}(q^2)\tau A_{\mu}(q) = -ie\bar{\tau}\left[\gamma^{\mu}F_1(q^2) + \frac{i\sigma^{\mu\nu}q_{\nu}}{2m_{\tau}}F_2(q^2) + \frac{\sigma^{\mu\nu}\gamma_5 q_{\nu}}{2m_{\tau}}F_3(q^2)\right]\tau A_{\mu}(q), \tag{1.1}$$

which defines the magnetic and electric dipole moments as

$$a_{\tau} = F_2(0) \quad \text{and} \quad d_{\tau} = \frac{e}{2m_{\tau}}F_3(0), \tag{1.2}$$

as well as the mean squared radius

$$\langle \vec{r}^2 \rangle = -6\frac{dG_E}{d\vec{q}^2}\bigg|_{q^2=0}, \tag{1.3}$$

with

$$G_E(q^2) = F_1(q^2) + \frac{q^2}{4m_{\tau}^2}F_2(q^2). \tag{1.4}$$

We take the form factors $F_{2,3}(q^2)$ at the leading order for $q^2 \to 0$, while we retain the first order in q^2 for the form factor $F_1(q^2)$.

The photon mediating the process $e^+e^- \to \tau^+\tau^-$ at Belle II is not on shell and the definitions above only apply if the difference between the form factors at $q^2 \neq 0$ and their values at $q^2 = 0$ is sufficiently small. This is expected to be the case unless there is a threshold nearby. Nevertheless, the reader should bear in mind that our limits—as well as all the quoted ones—are actually for the momentum-dependent form factors $F_i(s)$, with $\sqrt{s}$ the center-of-mass energy of the process—about 10 GeV at the Belle II experiment.

Whereas the magnetic moments of lighter leptons are measured to an accuracy that probes the respective radiative contributions expected within the SM, that of the heavier τ lepton is still only known to a lower precision: the current limits [2]

$$-0.052 < a_{\tau} < 0.013 \quad (95\%)\ \text{CL}, \tag{1.5}$$

are one order of magnitude above the theoretical value [3]

$$a_\tau^{\mathrm{SM}} = 1.17721(5) \times 10^{-3}. \tag{1.6}$$

The electric dipole moment is constrained to be (with an integrated luminosity of 833 fb^{-1}) [4]

$$-0.185 \times 10^{-16} < d_\tau < 0.061 \times 10^{-16}\ \mathrm{e\,cm} \quad (95\%)\ \mathrm{CL} \tag{1.7}$$

assuming its value to be real. A nonvanishing value would signal the presence of CP violation.

No direct limits on the electromagnetic radius of the τ lepton exist, but there is a bound on the scale [5]

$$\Lambda_{\mathrm{C.I.}} > 7.9\ \mathrm{TeV} \tag{1.8}$$

for the related four-fermion contact interaction (C.I.)

$$+\frac{2\pi}{\Lambda^2_{\mathrm{C.I.}}}(\bar{e}_L\gamma^\mu e_L)(\bar{\tau}_L\gamma_\mu\tau_L), \tag{1.9}$$

constrained at the energy of about 200 GeV.

The form factors introduced in Eq. (1.1) translate, in the language of effective field theory, into the $SU(2) \times U(1)$-invariant effective operators for the τ lepton. The leading contributions come from the following three higher-dimensional operators:

$$\hat{O}_1 = e\frac{c_1}{m_\tau^2}\bar{\tau}\gamma^\mu\tau D^\nu F_{\mu\nu}, \qquad \hat{O}_2 = e\frac{c_2 v}{2m_\tau^2}\bar{\tau}\sigma^{\mu\nu}\tau F_{\mu\nu},$$
$$\text{and} \quad \hat{O}_3 = e\frac{c_3 v}{2m_\tau^2}\bar{\tau}\sigma^{\mu\nu}\gamma_5\tau F_{\mu\nu}, \tag{1.10}$$

where D^ν is the covariant derivative, $F_{\mu\nu}$ is the electromagnetic field strength tensor, and $v = 174$ GeV is the Higgs field vacuum expectation value. In Eq. (1.10) the dimensionless Wilson coefficients c_i are taken to be real. Left- and right-handed chiral fields enter symmetrically. The operator $\hat{O}_1$ gives the leading q^2 dependence of the form factor F_1, while $\hat{O}_{2,3}$ give the q^2-independent term of the form factors $F_{2,3}$,

$$F_1(q^2) = 1 + c_1\frac{q^2}{m_\tau^2} + \ldots \quad \text{and} \quad F_{2,3}(0) = 2c_{2,3}\frac{v}{m_\tau}. \tag{1.11}$$

The operators $\hat{O}_{2,3}$ are written for the sake of convenience with an extra factor v/m_τ, sourced after the electroweak symmetry breaking by the dimension-six $SU(2)_L \times U(1)_Y$ gauge-invariant operators involving the Higgs field. Operators of higher dimensions can, in general, contribute—they give further terms in the expansion of the form factors—but their effect is suppressed.

Compared to the effective field theory approach, the form factors we use have the advantage of directly answering a simple question: is the τ lepton a pointlike particle or does it show a composite structure? The answer comes without relying on any assumption or UV model to select the relevant operators out of the many present in the effective theory.

Our strategy to constrain the electromagnetic couplings in Eq. (1.1) exploits the polarization density matrix, which can be experimentally reconstructed through a procedure dubbed "quantum tomography" and gives a bird's-eye view of the possible observables available for a given process. The method has been previously used to constrain physics beyond the SM affecting the top-quark [6,7] and τ-pair [7] production at the LHC or yielding Higgs anomalous couplings to τ leptons [8] and gauge bosons [9–11]. For the present case, we use the entries of the polarization density matrix to define three observables that provide the means to best constrain the parameters in Eq. (1.1): one observable measures the entanglement [12] in the spin states of the produced τ pairs, another is related to triple products involving one momentum and the spin vectors of the τ leptons—and it is specific to the CP-violating electric dipole moment, and the third is the total cross section.

We compare our results to the current experimental limits [13] and to recent phenomenological estimates of the electric and magnetic dipole moments in [14,15] and of the electric dipole moments in [16].

Proposals to measure the electric and magnetic dipole momenta of the τ lepton by exploiting polarized beams at B factories are discussed in Refs. [17,18].

A. Events

We propose to probe the electromagnetic couplings of the τ lepton by using the process $e^+e^- \to \tau^+\tau^-$ at the Belle II experiment, located at the SuperKEKB collider. The SuperKEKB collider delivers e^+e^- collisions at a center-of-mass energy of $\sqrt{s} = 10.579$ GeV. The Belle Collaboration has published analyses of $e^+e^- \to \tau^+\tau^-$ production with data corresponding to an integrated luminosity of up to 921 fb^{-1} [19], equivalent to 841×10^6 $\tau^+\tau^-$ events, and other 175×10^6 events have now been added with the Belle II dataset [20]. The aim of the SuperKEKB project is to collect 50 ab^{-1} of data [1,21], corresponding to a dataset of about 50×10^9 $e^+e^- \to \tau^+\tau^-$ events. Of these, we can use those involving the $\tau^- \to \pi^-\nu_\tau$, $\tau^- \to \pi^-\pi^0\nu_\tau$, and $\tau^- \to \pi^-\pi^+\pi^-\nu_\tau$ decays to reconstruct the polarization density matrix. The combination of these channels covers about 21% of τ-pair decays.

We expect the dominant background to arise from misreconstructions of the τ decay channel, affecting about 15% of the $e^+e^- \to \tau^+\tau^-$ events at Belle II [20]. Backgrounds arising from the process $e^+e^- \to \mathrm{q\bar{q}}$ and from other sources are negligible in comparison. Given their modest impact, we neglect the effect of backgrounds in our study. It will have to be taken into account when the analysis is performed on the actual data.

The detailed Monte Carlo simulation of the process $e^+e^- \to \tau^+\tau^-$ in [22] shows that a full quantum tomography is achievable and provides an indication of the uncertainties in the density matrix that we are going to use in our analysis. This simulation only provides an estimate of the statistical uncertainties. A more refined result accounting for complete background selections and realistic detector effects can only be obtained by the experimental collaboration.

II. METHODS

Quantum tomography aims to fully determine the density matrix ρ of a quantum state. The τ leptons—whose spins are represented with two-level quantum states, that is, "qubits"—act as their own polarimeters and the full polarization density matrix can be reconstructed, within the inherent uncertainties of the procedure, from the angular distribution of the τ decay products.

The polarization density matrix is very sensitive to any departure from the SM limit. Deviations are encoded in correlations and entanglement—whose study may provide a powerful probe into the presence of physics beyond the SM. The use of entanglement to study new physics in high-energy scattering has been pioneered in a number of recent works. The review in [23] summarizes these results and provides an introduction to the details of the procedure in the case of $e^+e^- \to \tau^+\tau^-$ and other processes.

Polarizations are more difficult to measure than momenta and so the reconstruction of the polarization density matrix from the data is challenging. The main aim of this work is to show to what extent the advantages of using the proposed method make the extra work in the experimental analysis eventually worthwhile.

The density matrix describing the polarization state of a quantum system composed by two fermions can be written as

$$\rho = \frac{1}{4}\Big[\mathbb{1}\otimes\mathbb{1} + \sum_i \mathrm{B}_i^+(\sigma_i\otimes\mathbb{1}) + \sum_j \mathrm{B}_j^-(\mathbb{1}\otimes\sigma_j) + \sum_{i,j}\mathrm{C}_{ij}(\sigma_i\otimes\sigma_j)\Big], \tag{2.1}$$

where $i,j \in \{n,r,k\}$ and σ_i are the Pauli matrices. The decomposition refers to a right-handed orthonormal basis $\{\hat{\mathbf{n}},\hat{\mathbf{r}},\hat{\mathbf{k}}\}$ and the quantization axis for the polarization is taken along $\hat{\mathbf{k}}$, so that $\sigma_k \equiv \sigma_3$. In the fermion-pair center-of-mass frame, we have

$$\hat{\mathbf{n}} = \frac{1}{\sin(\theta)}(\hat{\mathbf{p}}\times\hat{\mathbf{k}}), \quad \hat{\mathbf{r}} = \frac{1}{\sin(\theta)}(\hat{\mathbf{p}} - \cos(\theta)\hat{\mathbf{k}}), \tag{2.2}$$

where $\hat{\mathbf{k}}$ is the direction of the τ^+ momentum and θ is the scattering angle satisfying $\hat{\mathbf{p}}\cdot\hat{\mathbf{k}} = \cos\theta$, with $\hat{\mathbf{p}}$ being the direction of the incoming e^+.

The coefficients $\mathrm{B}_i^\pm$ in Eq. (2.1) give the polarizations of the individual fermions, whereas the matrix C_{ij} contains the spin correlations. By using the properties $\mathrm{Tr}(\sigma_i\sigma_j) = 2\delta_{ij}$ and $\mathrm{Tr}(\sigma_i) = 0$, we have

$$\mathrm{B}_i^+ = \mathrm{Tr}[\rho(\sigma_i\otimes\mathbb{1})], \qquad \mathrm{B}_i^- = \mathrm{Tr}[\rho(\mathbb{1}\otimes\sigma_i)], \qquad \mathrm{C}_{ij} = \mathrm{Tr}[\rho(\sigma_i\otimes\sigma_j)], \tag{2.3}$$

and, for the process at hand, it holds that $\mathrm{B}_i^\pm = 0$.

The nonvanishing coefficients C_{ij} can be reconstructed in the actual experiments by tracking the angular distribution of suitable τ-pair decay products. In particular, for events where each τ lepton decays to a single pion and a neutrino, we have

$$\frac{1}{\sigma}\frac{d\sigma}{d\cos\theta_i^+ d\cos\theta_j^-} = \frac{1}{4}\left(1 + \mathrm{C}_{ij}\cos\theta_i^+\cos\theta_j^-\right), \tag{2.4}$$

where $\cos\theta_i^\pm$ is the projections of the $\pi^\pm$ momentum direction on the $\{\hat{\mathbf{n}},\hat{\mathbf{r}},\hat{\mathbf{k}}\}$ basis, as computed in the rest frame of the decaying $\tau^\pm$. Crucial to the whole procedure is the reconstruction of the neutrino kinematics. More details pertaining to the experimental determination of the C_{ij} coefficients for different decay channels are presented, for instance, in Ref. [22], which we closely follow.

Quantum tomography gives the coefficients B_i and C_{ij} for the density matrix and there are a number of observables that can be constructed with them. We consider the three that provide the most stringent limits on the anomalous couplings:

(i) The concurrence $\mathscr{C}[\rho]$ [12] is a direct measure of entanglement in a system. It can be computed in our case by means of the particularly simple formula

$$\mathscr{C}[\rho] = \frac{1}{2}\max\Big[0, |\mathrm{C}_{rr} + \mathrm{C}_{kk}| - (1 + \mathrm{C}_{nn}), \sqrt{(\mathrm{C}_{rr} - \mathrm{C}_{kk})^2 + 4\mathrm{C}_{rn}^2} - |1 - \mathrm{C}_{nn}|\Big], \tag{2.5}$$

because the $B_i^\pm = 0$ and all off-diagonal elements but C_{rn} vanish when the scattering angle is integrated over. We use as first observable the concurrence in Eq. (2.5) computed from the C matrix obtained by averaging over the angular distribution of the τ leptons.

(ii) The second observable is just the total cross section

$$\sigma = \frac{1}{64\pi^2 s}\int d\Omega \frac{|\mathcal{M}|^2}{4}\sqrt{1 - \frac{4m_\tau^2}{s}}, \tag{2.6}$$

where we neglect the electron mass and $\sqrt{s} = 10.579$ GeV. The spin-summed squared amplitude $|\mathcal{M}|^2$ is given by

$$|\mathcal{M}|^2 = e^4\left\{\frac{s}{m_\tau^2}\left[\sin^2\theta\left(16c_1^2+\tilde{d}_\tau^2+a_\tau^2\right)+4c_1(\cos 2\theta+4a_\tau+3)\right]+2\frac{s^2}{m_\tau^4}c_1^2(\cos 2\theta+3)\right.$$
$$\left.+4\left(8c_1\sin^2\theta+\left(\tilde{d}_\tau^2+a_\tau^2+1\right)\cos^2\theta-\tilde{d}_\tau^2+a_\tau^2+4a_\tau+1\right)+16\frac{m_\tau^2}{s}\sin^2\theta\right\}. \quad (2.7)$$

(iii) The third observable $\mathscr{C}_{\rm odd}$ singles out the antisymmetric parts of the density matrix. It is defined as

$$\mathscr{C}_{\rm odd} = \frac{1}{2}\sum_{i,j<j}|\mathrm{C}_{ij}-\mathrm{C}_{ji}| \quad (2.8)$$

and contains only off-diagonal terms that change sign under transposition. The observable encodes kinematical variables that can be written as the triple products of momenta and spin vectors, for instance,

$$\vec{k}\cdot(\vec{s}_{\hat{n}}\times\vec{s}_{\hat{r}}), \quad (2.9)$$

where $\vec{k}$ is the momentum of one of the particles, and $\vec{s}_{\hat{n}}$ and $\vec{s}_{\hat{r}}$ are the projections of the spin vector along two directions orthogonal to the momentum. In the present case, there is only one nonvanishing term coming from the elements C_{rn} and C_{nr}, which are equal in magnitude and with the opposite sign. We build the observable $\mathscr{C}_{\rm odd}$ from the C matrix obtained by averaging over the angular distribution of the τ leptons.

The integration over the angular distribution used for the operators $\mathscr{C}[\rho]$ and $\mathscr{C}_{\rm odd}$ is performed over the range defined by $|\cos\theta| < 0.4$ to optimize the quantum tomography procedure.

A. Uncertainties

To set limits on the parameters in Eq. (1.1) we need to know the uncertainties of the operators we utilize to characterize the process $e^+e^-\to\tau^+\tau^-$ at Belle II. These have been estimated for a benchmark luminosity of 1 ab^{-1} as follows. For the concurrence $\mathscr{C}[\rho]$ and the CP odd operator $\mathscr{C}_{\rm odd}$, we rescale the corresponding uncertainties of 1.4×10^{-3} and 4.0×10^{-3} given in Ref. [22] (after averaging on the angular distribution of τ leptons) for a luminosity of 220 fb^{-1} and for a center-of-mass energy $\sqrt{s}=10.579$ GeV. For the total cross section, instead, we rescale the relative uncertainty of 0.3% on the integrated luminosity quoted in Ref. [24] for 833 fb^{-1}. All these uncertainties are at the 1σ confidence level and contain (to different extents) also statistical errors due to the effect of initial state radiation on the energy and the imperfect reconstruction of the momenta.

III. RESULTS

The operators introduced in the previous section, generically denoted here as $\mathscr{O}_i(a_\tau,d_\tau,c_1)$, depend on the electromagnetic couplings a_τ, d_τ, and c_1, and $\mathscr{O}_i(0,0,0)$ are the values of the operators for the SM. To constrain the couplings, we introduce a χ^2 test set for a (68.3) 95% joint CL,

$$\sum_i\left[\frac{\mathscr{O}_i(a_\tau,d_\tau,c_1)-\mathscr{O}_i(0,0,0)}{\sigma_i}\right]^2 \le (2.30)\,5.99, \quad (3.1)$$

in which we set the uncertainties σ_i for the operators $\mathscr{O}_i$ at the values discussed in the previous section.

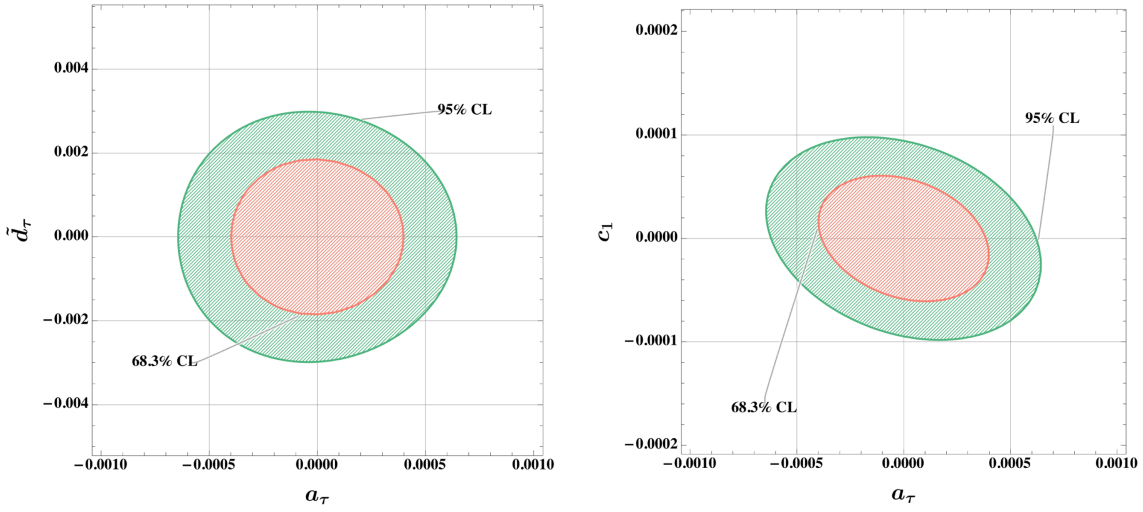

FIG. 1. Bounds on the electromagnetic couplings $a_\tau, \tilde{d}_\tau = F_3(0)$ and c_1 obtained by means of Eq. (3.1) varying two parameters at a time.

TABLE I. Bounds obtained on the single parameter after marginalization of the 95% joint confidence intervals for the electromagnetic couplings shown in Fig. 1, neglecting correlations. The values refer to a luminosity of 1 ab^{-1} at Belle II; limits for higher luminosities can be (approximately) obtained by rescaling these values by the square root of the ratio of the relative luminosities. The current experimental limits are reported in the first column.

PDG (2022)	This work
$-1.9\times10^{-17}\le d_\tau\le 6.1\times10^{-18}$ e cm	$\lvert d_\tau\rvert\le 1.7\times10^{-17}$ e cm
$-5.2\times10^{-2}\le a_\tau\le 1.3\times10^{-2}$	$\lvert a_\tau\rvert\le 6.3\times10^{-4}$
$\Lambda_{\mathrm{C.I.}}\ge 7.9$ TeV	$\lvert c_1\rvert\le 9.5\times10^{-5}$, $\Lambda_{\mathrm{C.I.}}\ge 2.6$ TeV

The operators $\mathscr{O}_i$ in Eq. (3.1) that we utilize to constrain a_τ and d_τ are $\mathscr{C}[\rho]$ and $\mathscr{C}_{\mathrm{odd}}$. We employ instead $\mathscr{C}[\rho]$ and the cross section σ to constrain a_τ and c_1.

The bounds on each coupling can be extracted from Fig. 1 via marginalization by assuming the parameters to be independent. The values obtained from the 95% joint confidence interval are reported in Table I, where they are compared to current experiment bounds.

A comparison between the effectiveness in probing the electromagnetic structure of the τ leptons of the entanglement and the cross section is now possible. The concurrence provides, for a common uncertainty, a limit 20% stronger than that given by the total cross section in determining the anomalous magnetic moment, as shown in Fig. 2. Whether this improvement in the constraint justifies the extra work required by quantum tomography depends on the details of the experimental setup. The method is beneficial only as long as the error in the cross section measurement is about the same size as the corresponding uncertainty in the determination of the τ-lepton polarizations.

On the other hand, the electric dipole moment limit is dominated by the observable $\mathscr{C}_{\mathrm{odd}}$, which is essentially the same as those used in other analyses, and comparable constraints are to be expected.

The radius of the τ lepton that can be explored is estimated from our limit on c_1 and Eq. (1.4) as

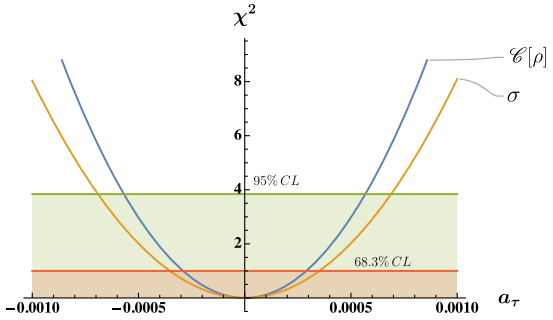

FIG. 2. Comparison between the power of entanglement (blue line) and cross section (orange line) to constrain the electromagnetic couplings. For the plot we use a common relative uncertainty of 0.1%. The green and red areas denote the 95% and 68.3% one-parameter confidence level, respectively.

$$\langle\vec{r}^2\rangle=\frac{6}{m_\tau^2}\left(c_1+\frac{a_\tau}{4}\right), \tag{3.2}$$

which gives the root-mean-squared radius value of

$$\sqrt{\langle\vec{r}^2\rangle}<5.1\times10^{-3}\ \mathrm{fm}. \tag{3.3}$$

By comparison, the electron, which is believed to be a pointlike particle, has a limit on its root-mean-squared radius of about 10^{-5} fm [25] that does not originate in radiative corrections.

IV. OUTLOOK

We have outlined a strategy to constrain the electric and magnetic dipole moments of the τ lepton, as well as its electromagnetic radius, via quantum tomography.

In order to put our results into perspective, we compute the single-parameter 68.3% confidence intervals for a_τ and d_τ from Eq. (3.1) and compare the resulting limits to those in the literature. With a luminosity of 1 ab^{-1}, Ref. [14] finds

$$\begin{aligned}&\lvert d_\tau-d_\tau^{\mathrm{SM}}\rvert<1.44\times10^{-18}\ \mathrm{e\,cm}\\ &\text{and}\quad \lvert a_\tau-a_\tau^{\mathrm{SM}}\rvert<1.24\times10^{-4}\end{aligned} \tag{4.1}$$

at 68.3% CL. Our method instead yields

$$\lvert d_\tau\rvert<6.7\times10^{-18}\ \mathrm{e\,cm}\quad\text{and}\quad\lvert a_\tau-a_\tau^{\mathrm{SM}}\rvert<2.6\times10^{-4}. \tag{4.2}$$

The SM prediction for d_τ^{SM} is still negligible at this precision level and so the first limit can be compared directly to ours. The SM prediction for a_τ^{SM} is given in Eq. (1.6) and therefore the limit in [14] is of the same order of magnitude as our result. Comparable results are obtained in Ref. [15] by using a combination of differential cross sections.

Reference [16] quotes the following 68.3% confidence interval for the electric dipole moment

$$\lvert d_\tau\rvert<6.8\times10^{-20}\ \mathrm{e\,cm}, \tag{4.3}$$

given for a luminosity of 50 ab^{-1}. Rescaling the result we obtained to account for the latter, we find

$$|d_\tau| < 9.4 \times 10^{-19}\ \text{e cm}. \tag{4.4}$$

It is not surprising that both the limits on the electric dipole moment reported in Refs. [14,16] are comparable to ours: these results are all obtained by using an operator involving the triple product of two spin vectors and one momentum, equivalent to the *CP* odd operator utilized in our analysis. The limit in Eq. (4.3) is stronger because of the smaller uncertainty used, which is obtained by combining in quadrature the yields of different decay channels. Our result, in fact, is comparable to those obtained in Ref. [16] for any single channel.

As for the bound obtained for the compositeness scale, see Table I, one has to bear in mind that the current experimental limit is obtained considering energies of about 200 GeV, whereas ours is given for energies one order of magnitude smaller, of about 10 GeV. Depending on the origin of the relevant four-fermion interaction, the scaling of the related operator is at least linear in the energy, implying that our result must be compared with the approximated rescaled value $\Lambda_{\text{C.I.}} \gtrsim 800$ GeV when assessing the power of the method.

ACKNOWLEDGMENTS

We are happy to thank E. Gabrielli, C. Veelken, and L. Zani for discussions. L. M. is supported by the Estonian Research Council grants PRG803, RVTT3 and by the CoE program grant TK202 "Fundamental Universe".

[1] W. Altmannshofer *et al.* (Belle II Collaboration), The Belle II physics book, Prog. Theor. Exp. Phys. **2019**, 123C01 (2019); **2020**, 029201(E) (2020).
[2] J. Abdallah *et al.* (DELPHI Collaboration), Study of tau-pair production in photon-photon collisions at LEP and limits on the anomalous electromagnetic moments of the tau lepton, Eur. Phys. J. C **35**, 159 (2004).
[3] S. Eidelman and M. Passera, Theory of the tau lepton anomalous magnetic moment, Mod. Phys. Lett. A **22**, 159 (2007).
[4] K. Inami *et al.* (Belle Collaboration), An improved search for the electric dipole moment of the τ lepton, J. High Energy Phys. 04 (2022) 110.
[5] S. Schael *et al.* (ALEPH Collaboration), Fermion pair production in e^+e^- collisions at 189–209-GeV and constraints on physics beyond the standard model, Eur. Phys. J. C **49**, 411 (2007).
[6] R. Aoude, E. Madge, F. Maltoni, and L. Mantani, Quantum SMEFT tomography: Top quark pair production at the LHC, Phys. Rev. D **106**, 055007 (2022).
[7] M. Fabbrichesi, R. Floreanini, and E. Gabrielli, Constraining new physics in entangled two-qubit systems: Top-quark, tau-lepton and photon pairs, Eur. Phys. J. C **83**, 162 (2023).
[8] M. M. Altakach, P. Lamba, F. Maltoni, K. Mawatari, and K. Sakurai, Quantum information and *CP* measurement in $H \to \tau^+\tau^-$ at future lepton colliders, Phys. Rev. D **107**, 093002 (2023).
[9] M. Fabbrichesi, R. Floreanini, E. Gabrielli, and L. Marzola, Stringent bounds on HWW and HZZ anomalous couplings with quantum tomography at the LHC, J. High Energy Phys. 09 (2023) 195.
[10] A. Bernal, P. Caban, and J. Rembieliński, Entanglement and Bell inequalities violation in $H \to ZZ$ with anomalous coupling, Eur. Phys. J. C **83**, 1050 (2023).
[11] R. Aoude, E. Madge, F. Maltoni, and L. Mantani, Probing new physics through entanglement in diboson production, J. High Energy Phys. 12 (2023) 017.
[12] R. Horodecki, P. Horodecki, M. Horodecki, and K. Horodecki, Quantum entanglement, Rev. Mod. Phys. **81**, 865 (2009).
[13] R. L. Workman *et al.* (Particle Data Group), Review of particle physics, Prog. Theor. Exp. Phys. **2022**, 083C01 (2022).
[14] X. Chen and Y. Wu, Search for the electric dipole moment and anomalous magnetic moment of the tau lepton at tau factories, J. High Energy Phys. 10 (2019) 089.
[15] U. Haisch, L. Schnell, and J. Weiss, LHC tau-pair production constraints on a_τ and d_τ, SciPost Phys. **16**, 048 (2024).
[16] W. Bernreuther, L. Chen, and O. Nachtmann, Electric dipole moment of the tau lepton revisited, Phys. Rev. D **103**, 096011 (2021).
[17] J. Bernabéu, G. González-Sprinberg, J. Papavassiliou, and J. Vidal, Tau anomalous magnetic moment form factor at super b/flavor factories, Nucl. Phys. **B790**, 160 (2008).
[18] A. Crivellin, M. Hoferichter, and J. M. Roney, Toward testing the magnetic moment of the tau at one part per million, Phys. Rev. D **106**, 093007 (2022).
[19] D. Sahoo *et al.* (Belle Collaboration), Search for lepton-number- and baryon-number-violating tau decays at Belle, Phys. Rev. D **102**, 111101 (2020).
[20] Belle II Collaboration, Measurement of the τ-lepton mass with the Belle II experiment, Phys. Rev. D **108**, 032006 (2023).
[21] SuperKEKB Collaboration, SuperKEKB collider, Nucl. Instrum. Methods Phys. Res., Sect. A **907**, 188 (2018).
[22] K. Ehatäht, M. Fabbrichesi, L. Marzola, and C. Veelken, Probing entanglement and testing Bell inequality violation with $e + e - \tau + \tau -$ at Belle II, Phys. Rev. D **109**, 032005 (2024).

[23] A. J. Barr, M. Fabbrichesi, R. Floreanini, E. Gabrielli, and L. Marzola, Quantum entanglement and Bell inequality violation at colliders, arXiv:2402.07972.

[24] S. Banerjee, B. Pietrzyk, J. M. Roney, and Z. Was, Tau and muon pair production cross-sections in electron-positron annihilations at $\sqrt{s} = 10.58$-GeV, Phys. Rev. D **77**, 054012 (2008).

[25] D. Bourilkov, Hint for axial vector contact interactions in the data on $e^+e^- \to e^+e^-(\gamma)$ at center-of-mass energies 192–208 GeV, Phys. Rev. D **64**, 071701 (2001).